

# GASEOUS EFFLUENT TREATMENT USING A PULSED CORONA DISCHARGE

Michael G. Grothaus  
Southwest Research Institute  
6220 Culebra Road  
San Antonio, TX 78228-0510

R. Kenneth Hutcherson, Richard A. Korzekwa\*, Russel Brown,  
Michael W. Ingram\*\*, Randy Roush  
Dahlgren Division  
Naval Surface Warfare Center  
17320 Dahlgren Road  
Dahlgren, VA 22448-5100

Scott E. Beck, Mark George, Rick Pearce, Robert G. Ridgeway  
Air Products and Chemicals, Inc.  
7201 Hamilton Boulevard  
Allentown, PA 18195-1501

## Abstract

A pulsed corona reactor (PCR) has been investigated for the abatement of a variety of hazardous gaseous compounds including volatile organic compounds, chlorofluorocarbons, perfluorinated compounds and oxides of nitrogen. In this technique, a series of fast-risetime, high-voltage pulses are applied to a wire-cylinder geometry resulting in a plethora of streamer discharges within an atmospheric pressure flowing gas volume. This non-thermal plasma can be particularly effective in treating dilute concentrations of pollutant compounds where power consumption is of prime concern. Such conditions exist in a variety of situations including chemical warfare threat scenarios, semiconductor processing, and mobile sources. In order to assess the value of such a technology as a solution to practical applications, a complete analysis of reactor operation must be performed, including "wall-plug" efficiency and by-product identification.

The Dahlgren Laboratory of the Naval Surface Warfare Center, Air Products and Chemicals, Inc., and Southwest Research Institute have investigated the abatement efficacy of a prototype coaxial PCR for a variety of chemical compounds including  $C_7H_8$ ,  $CCl_2F_2$ ,  $CH_2Cl_2$ ,  $CH_3CCl_3$ ,  $NF_3$ ,  $SF_6$ ,  $C_2F_6$  and  $NO_x$ . Operation of a 10-tube reactor operation has been carefully analyzed under a variety of flow conditions and pulse parameters (specifically voltages to 35 kV, rep-rates to 1.5 kHz, flow rates to 50 slpm, pulse-widths less than 150 ns). Each situation can be compared using the preferred Joules/liter specification. By-products emanating from the reactor have been analyzed using near "real-time" mass spectrometry. Results of a series of such experiments as well as future directions and areas of concern will be presented.

---

\*Currently at Los Alamos National Laboratory, Los Alamos, NM.

\*\*Currently at Physics International, San Leandro, CA.

## Report Documentation Page

*Form Approved*  
*OMB No. 0704-0188*

Public reporting burden for the collection of information is estimated to average 1 hour per response, including the time for reviewing instructions, searching existing data sources, gathering and maintaining the data needed, and completing and reviewing the collection of information. Send comments regarding this burden estimate or any other aspect of this collection of information, including suggestions for reducing this burden, to Washington Headquarters Services, Directorate for Information Operations and Reports, 1215 Jefferson Davis Highway, Suite 1204, Arlington VA 22202-4302. Respondents should be aware that notwithstanding any other provision of law, no person shall be subject to a penalty for failing to comply with a collection of information if it does not display a currently valid OMB control number.

1. REPORT DATE <b>JUL 1995</b>	2. REPORT TYPE <b>N/A</b>	3. DATES COVERED <b>-</b>	
4. TITLE AND SUBTITLE <b>Gaseous Effluent Treatment Using A Pulsed Corona Discharge</b>		5a. CONTRACT NUMBER	
		5b. GRANT NUMBER	
		5c. PROGRAM ELEMENT NUMBER	
6. AUTHOR(S)		5d. PROJECT NUMBER	
		5e. TASK NUMBER	
		5f. WORK UNIT NUMBER	
7. PERFORMING ORGANIZATION NAME(S) AND ADDRESS(ES) <b>Southwest Research Institute 6220 Culebra Road San Antonio, TX 78228-0510</b>		8. PERFORMING ORGANIZATION REPORT NUMBER	
9. SPONSORING/MONITORING AGENCY NAME(S) AND ADDRESS(ES)		10. SPONSOR/MONITOR'S ACRONYM(S)	
		11. SPONSOR/MONITOR'S REPORT NUMBER(S)	
12. DISTRIBUTION/AVAILABILITY STATEMENT <b>Approved for public release, distribution unlimited</b>			
13. SUPPLEMENTARY NOTES <b>See also ADM002371. 2013 IEEE Pulsed Power Conference, Digest of Technical Papers 1976-2013, and Abstracts of the 2013 IEEE International Conference on Plasma Science. Held in San Francisco, CA on 16-21 June 2013. U.S. Government or Federal Purpose Rights License.</b>			
14. ABSTRACT <b>pulsed corona reactor (PCR) has been investigated for the abatement of a variety of hazardous gaseous compounds including volatile organic compounds, chlorofluorocarbons, perfluorinated compounds and oxides of nitrogen. In this technique, a series of fast-rise time, high-voltage pulses are applied to a wire-cylinder geometry resulting in a plethora of streamer discharges within an atmospheric pressure flowing gas volume. This non-thermal plasma can be particularly effective in treating dilute concentrations of pollutant compounds where power consumption is of prime concern. Such conditions exist in a variety of situations including chemical warfare threat scenarios, semiconductor processing, and mobile sources. In order to assess the value of such a technology as a solution to practical applications, a complete analysis of reactor operation must be performed, including "wall-plug" efficiency and by-product identification.</b>			
15. SUBJECT TERMS			
16. SECURITY CLASSIFICATION OF:			17. LIMITATION OF ABSTRACT <b>SAR</b>
a. REPORT <b>unclassified</b>	b. ABSTRACT <b>unclassified</b>	c. THIS PAGE <b>unclassified</b>	
			18. NUMBER OF PAGES <b>9</b>
			19a. NAME OF RESPONSIBLE PERSON

## Introduction

Preventing or controlling hazardous gaseous substances from being emitted into the ambient environment has become a major focus of the scientific community in response to public pressure regarding the establishment and maintenance of healthful air standards. Compliance pressures are being exerted on both the military and industrial sectors in the form of increasingly stringent environmental regulations. Failure to comply with the provisions and amendments of the Clean Air Act of 1990, the Federal Facilities Compliance Act, and other international, federal and state air standards can result in costly fines and interruption of critical operations. Such potential consequences should presumably provide adequate incentive for investment in the development of alternative abatement technologies while more environmentally compatible chemical products and processes are developed and introduced into the marketplace. Of course, additional impetus can be associated with the recent emphasis on, and financial reapportionment to, the conversion and development of heretofore defense-related technologies for commercial applications.

Industrial processing applications involving the use or production of significant quantities of perfluorinated compounds (PFCs), chlorofluorocarbons (CFCs), and volatile organic compounds (VOCs) must now eliminate these compounds from their effluent gas streams. For example, gases such as  $\text{NF}_3$ ,  $\text{CF}_4$ ,  $\text{C}_2\text{F}_6$ ,  $\text{C}_3\text{F}_8$ ,  $\text{SF}_6$ ,  $\text{CCl}_2\text{F}_2$ , and  $\text{CHF}_3$  are used by the microelectronics industry in a variety of plasma based applications including plasma enhanced chemical vapor deposition, plasma etching, and plasma cleaning, while  $\text{CCl}_2\text{F}_2$ ,  $\text{C}_7\text{H}_8$ ,  $\text{CH}_2\text{Cl}_2$ , and  $\text{CH}_3\text{CCl}_3$  are found in other applications such as wafer cleans and oxidation enhancement. Many of these compounds are ozone depleters or are participants in postulated global warming mechanisms<sup>1</sup>. In general, only a small portion of these gases are actually consumed in a typical semiconductor fabrication process so that the effluent stream from a particular process may contain relatively large quantities of toxic and environmentally harmful species.

Current emission control methodologies (i.e. scrubbers) can produce undesirable by-products, or are not generally regarded as cost-effective, or can have other drawbacks associated with their integration into existing systems. Commercially available scrubbers typically utilize a combination of four different control technologies. These include wet, thermal, dry, or sub-atmospheric plasma techniques<sup>2</sup>. For example, thermal scrubbing entails mixing the process exhaust with hydrogen or oxygen and passing the mixture through a flame or ignitor where the effluent gases burn or crack. In a typical semiconductor manufacturing application, 50 standard liters per minute of one of these gases will be used, and since these scrubbers are employed in a continuous mode, this gas flow rate represents a significant cost to the semiconductor manufacturer. Additionally, there are safety and maintenance factors which must be addressed when using hydrogen, especially when it is mixed with oxygen to burn the effluent species. Plasma scrubbing is typically accomplished at a sub-atmospheric pressure (0.1 to 10 Torr) with the device installed between a process reaction chamber and the processing system's vacuum pump. At this location, the exhaust gases from the process reaction chamber pass through the plasma device where they are cracked. One problem encountered with this type of technique is that once the species are cracked they can have a high probability of recombining into their original form before they are exhausted from the facility. Solid phase by-products can also form within the processing reactor or the scrubber reactor and can deposit on the reactors' internal surfaces, back-diffuse toward the processing reactor or be swept from the reactor into the roughing pump. For wet scrubbers, limits on the solubility of the pollutant in the scrubbing liquid is of concern, as well as final disposal of the pollutant-saturated liquid.

Non-thermal atmospheric-pressure plasmas (e.g. pulsed corona discharge, silent discharge, or electron-beam discharge) are being investigated as potentially viable alternatives for the abatement of  $\text{NO}_x$ ,  $\text{SO}_x$ , VOCs, CFCs and PFCs<sup>3,4</sup>. Such plasmas show promise of being highly efficient, particularly in cases involving relatively dilute pollutant concentrations which are contained within a background gas matrix such as nitrogen or air (e.g. 100-1000 ppmv). Each of these discharges can be characterized by a mean electron energy which is considerably higher than that of the bulk-gas molecules, as opposed to thermal plasmas in which all the constituents are essentially in thermal equilibrium. The chemical efficiency of the approach stems from the fact that even though these electrons are relatively short-lived under atmospheric pressure conditions and rarely interact directly with the offending molecules, they do collide with the dominant background gas molecules, creating radical species. These radicals can have relatively long lifetimes and can react selectively with the pollutant molecules leading to their eventual neutralization as a threat. It is important to note that these reactions take place without a significant increase in the temperature of the background gas, which translates into a substantial energy savings over thermal methods.

Establishing the commercial and/or military viability of the non-thermal plasma approach will require not only the delineation of the device's chemical efficiency under a wide variety of conditions, but will require measurement of the "wall-plug" efficiency, identification of reaction by-products (harmful or otherwise), quantization of the device's reliability and maintainability, and a guarantee of a reasonable "cost-of-ownership." The present work describes a collaborative effort which was undertaken to investigate the efficacy of one such reactor, the pulsed corona discharge reactor (PCR), against a wide variety of pollutant molecules of interest to both the military and industrial sectors.

### Experimental Apparatus

The pulsed power driver was designed and constructed to optimize the electrical efficiency of the reactor without having to resort to complex, expensive, or load-sensitive power conditioning methodologies. As shown in Figure 1, a small capacitance,  $C_s$  (380 pF to 4 nF), is charged using a constant current power supply (Maxwell Model CCDS-250P1-208) thereby avoiding losses which will be encountered in constant voltage resistive charging schemes. The prototype module consists of ten 90 cm long, 2.5 cm diameter stainless steel tubes containing coaxially located 500  $\mu\text{m}$  diameter stainless steel wires. The reactor sub-modules operate in parallel by electrically connecting the center conductors of each to a common high voltage header plate. A high-pressure hydrogen filled spark gap<sup>5</sup> is placed between  $C_s$  and the reactor capacitance,  $C_r$ , as a peaking switch. No gas flow is required for the switch to operate. The capacitor

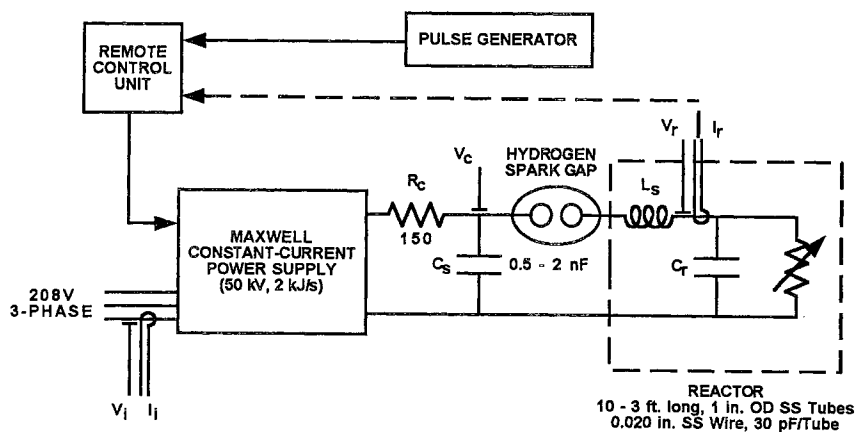


Figure 1. A schematic diagram of the pulsed corona reactor.

is connected to a common high voltage header plate. A high-pressure hydrogen filled spark gap<sup>5</sup> is placed between  $C_s$  and the reactor capacitance,  $C_r$ , as a peaking switch. No gas flow is required for the switch to operate. The capacitor

$C_s$  is charged in a linear manner until the self-breakdown voltage of the hydrogen spark gap is surpassed at which time a fast-rising pulse (few ns) is resonantly applied to the reactor through the stray inductance  $L_s$ . The coaxial hydrogen spark gap is constructed using ceramic insulators (Macor and alumina) to handle thermal stresses while Elkonite<sup>®</sup> electrodes are employed to minimize electrode erosion. Upon initiation of corona current, the power supply resonant inverter is disabled in order to prevent recharging of  $C_s$  and allow recovery of the spark gap, thus isolating the supply from the reactor. Corona current is extinguished as the energy in the small storage capacitance,  $C_s$ , is depleted, preventing the transition to a thermal arc condition. The repetition-rate of the system is controlled by an external pulse generator.

A cross-sectional view of one of the ten identical reactor tubes is shown in Figure 2. The 500  $\mu\text{m}$  diameter stainless steel (SS) electrode is positioned in the center of a 2.29 cm inner diameter SS tube by two perforated Teflon spacers and is held taut by a SS crimp and SS tensioning screw at either end. Teflon feedthroughs were used for all electrical connections, while a pressure seal is maintained by a specially constructed Teflon to Swagelok fitting.

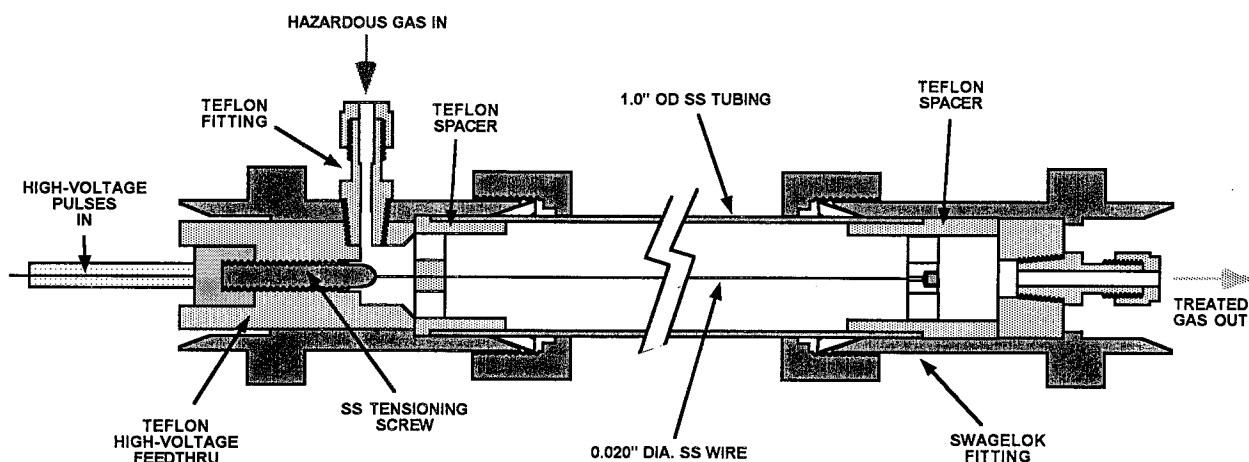


Figure 2. Cross-sectional view of an individual reactor tube. Materials in contact with the gas flow are either Teflon or stainless steel.

Fast electrical diagnostics are required to measure the applied pulse parameters in order to accurately determine the energy delivered to the reactor per unit gas volume (in units of Joules/liter). Such diagnostics should not significantly interfere with or affect the operation of the device. The energy per pulse is dependent not only on the storage capacitance value and charging voltage, but also on the residual voltage left on the reactor after the streamers have extinguished. A fast coaxial capacitive voltage divider, capable of sub-nanosecond risetimes, was used to measure the output voltage,  $V_r$ . The probe has a sensitivity of  $1.5\text{E-}5$  V/V with a decay time constant of  $5 \mu\text{s}$ . This time-constant is sufficient for measuring the corona pulse, however, the intra-pulse residual voltage must be measured using another, longer time constant probe. Since the spark gap has not recovered within the time span of the corona pulse (50-150 ns), the Tektronix voltage probe (Model 6015A) which is used to monitor the voltage on the energy store,  $C_s$ , can be used to determine the correct bias level. A  $1\text{-G}\Omega$  input impedance resistive divider was used to verify the Tektronix probe measurement. The residual voltage is then added to the  $V_r$  waveform to give the correct reactor voltage magnitude. The reactor current is monitored with a Pearson current probe, Model 2878 (2 ns risetime,  $0.1\text{V/A}$  sensitivity) or Model

4100 (10 ns risetime, 1V/A). The accuracy of all fast voltage and current probes was verified independently through the use of a 2 kV subnanosecond 50-ohm cable pulser. Thus obtained, the integrated product of the reactor voltage and current waveforms will yield the energy delivered per pulse. Power input to the switching supply is also monitored so that a complete "wall-plug" efficiency of the reactor scheme can be calculated.

The experimental setup for controlled introduction of the pollutant species and the analysis of the effluent from the pulsed corona reactor is shown in Figure 3. The carrier gas stream flow rate and moisture content is controlled with a Miller-Nelson relative humidity-temperature mass flow controller. The pollutant gases (e.g.  $\text{NF}_3$ ,  $\text{CCl}_2\text{F}_2$ ,  $\text{SF}_6$ ,  $\text{CF}_4$  and  $\text{C}_2\text{F}_6$ ) were supplied from gas cylinders where these were either 1% in  $\text{N}_2$  or 100% of the pollutant gas. A bubbler or syringe pump was used to supply

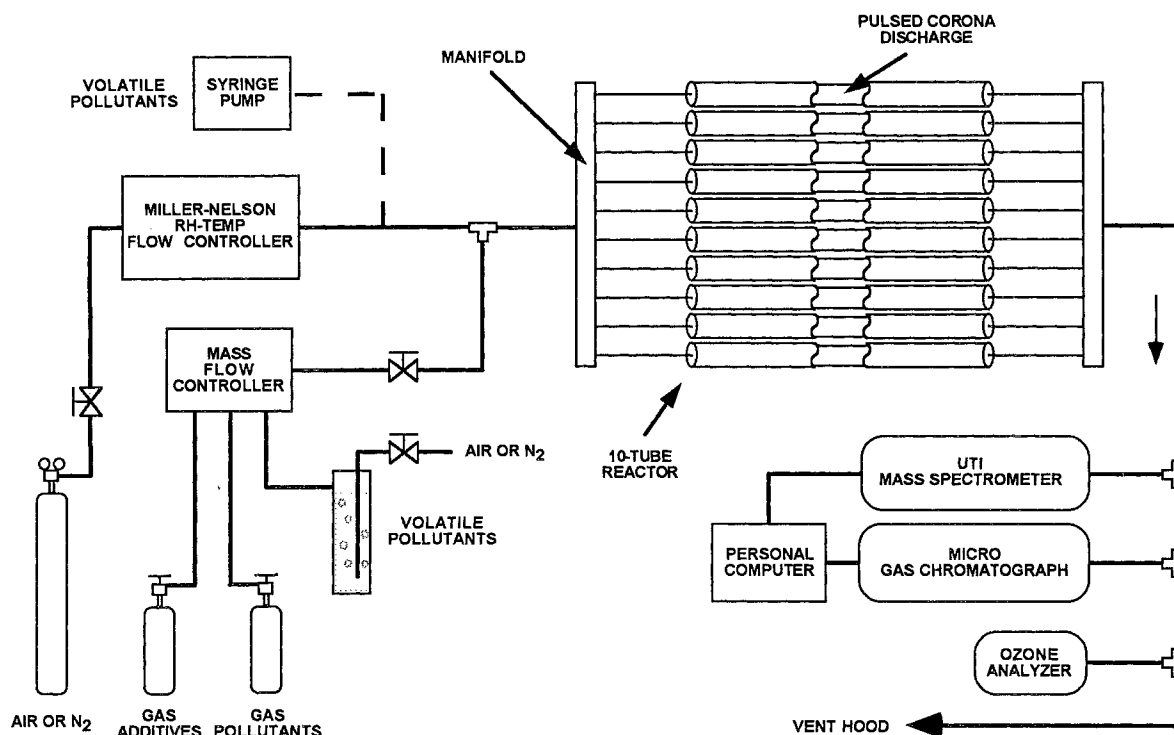


Figure 3. Chemical analysis testbed for characterization of the effluent emanating from the prototype pulsed corona reactor.

the volatiles such as  $\text{C}_7\text{H}_8$ ,  $\text{CH}_3\text{CCl}_3$  and  $\text{CH}_2\text{Cl}_2$ . Gases supplied to the bubbler included bottled air and  $\text{N}_2$ . Additive gases such as Ar, He,  $\text{O}_2$ , and  $\text{H}_2$  were available for measured introduction into the reactor gas volume. The pollutant gases were at times mixed with additive gases in a gas mixing manifold consisting of a series of Brooks Model 5850E mass flow controllers. Gas analysis was performed with a MTI Quad 400 gas chromatograph and a UTI QualiTrace mass spectrometer with a model 2221 probe.

### Experimental Results

The measured electrical characteristics at the input to the reactor appear typically as shown in the

correlated waveforms of Figure 4. The waveforms were acquired with the reactor operating at 10.2 standard liters per minute (slpm) of N<sub>2</sub> contaminated with 233 parts per million (ppm) of NF<sub>3</sub> and doped with 433 ppm H<sub>2</sub>. The waveforms represent an average of 100 discharges. The energy storage capacitance was measured at 380 pF. Figure 4a shows that the resonant voltage transfer from the prime store to the reactor is superimposed on the positive overdamped current pulse of the actual corona discharge. The voltage decays to a corona onset threshold of approximately 7 kV after the pulse. The absolute level of this threshold varies depending on the background gas mixture and reactor geometry and can result in secondary "DC" discharges within the intra-pulse period<sup>6</sup>. The risetime of the pulse was measured to be 6 ns with a total width of less than 100 ns. Energy delivered to the reactor shot (on average) was 100-200 mJ. Experimental emphasis was placed on minimizing the applied pulsewidth (fast risetime with minimum storage capacitance) in order to emphasize the effects due to the early phases of the streamer discharge development rather than the subsequent "driving" of the discharge towards more thermal conditions. This effect is demonstrated by the data in Table I showing the significant savings in required input energy density for a comparable reduction in pollutant concentration.

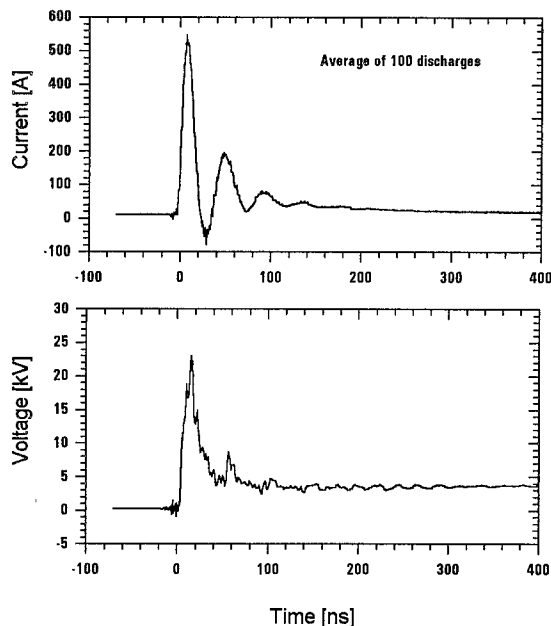


Figure 4. The electrical characteristics of the pulsed corona reactor where: (top) is the voltage applied to the reactor as measured by the fast capacitive probe, and (bottom) is the reactor current as measured by a Pearson current monitor.

The carrier gas containing the pollutant to be destroyed was found to play a significant role in the destruction of that pollutant. Although some applications will specifically require the exclusive use of ambient air, many industrial processes are not so constrained. Initial work with 330 ppm methylene chloride (CH<sub>2</sub>Cl<sub>2</sub>) in air at 35% relative humidity required 810 Joules per liter (J/l) to achieve a destruction efficiency of only 55%. Subsequent operation in a N<sub>2</sub> background with an input of 1020 J/l, the PCR was able to destroy the methylene chloride to a level below the detectable limits available from the gas chromatograph (GC) and mass spectrometer (MS). Table II demonstrates similar results for NF<sub>3</sub> and CF<sub>4</sub>.

Table I  
Energy Density vs. Reactor Configuration

93% Destruction of 250 ppm Toluene in Air				
Reactor Configuration	W/cfm	eV/molecule	J/liter	
3 TUBE REACTOR - 4 nF (0.4 CFM Flow)	230	420	412	
3 TUBE REACTOR - 2 nF (0.4 CFM Flow)	130	242	240	
10 TUBE REACTOR - 2 nF (1.8 CFM Flow)	63	124	115	
10 TUBE REACTOR - 1 nF (1.8 CFM Flow)	49	101	90	

The addition of reagent gases to the process stream were found to be beneficial in enhancing the destruction efficiencies of some compounds. Use of gettering gases,

Table II  
Changing Carrier Gas

Carrier Gas	Percent Removal		
	NF <sub>3</sub>	CH <sub>2</sub> Cl <sub>2</sub>	CF <sub>4</sub>
Air (80% N <sub>2</sub> , 20% O <sub>2</sub> )	7%	55%	--
N <sub>2</sub> + H <sub>2</sub> O (35% RH)	41%	--	--
Dry N <sub>2</sub>	38%	>99.9%	2%
Dry N <sub>2</sub> + H <sub>2</sub>	84%	--	4%
He + H <sub>2</sub>	--	--	32%
Reactor: 500 Hz, 100-200 mJ/pulse, 5-10 slpm			

Table III  
Achieved Destruction Efficiencies

Molecule	Removal Efficiency
NF <sub>3</sub>	>99.9%
C <sub>2</sub> F <sub>6</sub> (50% O <sub>2</sub> )	32%
SF <sub>6</sub>	72%
CF <sub>4</sub> (8% O <sub>2</sub> )	32%
CCl <sub>2</sub> F <sub>2</sub>	85%
C <sub>7</sub> H <sub>8</sub>	>99.9%
CH <sub>2</sub> Cl <sub>2</sub>	>99.9%
CH <sub>3</sub> CCl <sub>3</sub>	>99.9%

such as H<sub>2</sub>, has dramatically improved the destruction efficiency attainable for NF<sub>3</sub>. As in the case with the carrier gas, these additives may provide activated species which enhance the decomposition of halogenated compounds. Additives can also getter intermediate fluorine and chlorine atoms preventing recombination reactions which, in turn, leads to higher destruction efficiencies. Figure 5 shows the dependence of NF<sub>3</sub> removal on the relative concentration of an H<sub>2</sub> additive. The data was taken under constant reactor conditions of 1000 ppm NF<sub>3</sub> and 795 J/l being delivered to the gas volume. The enhancement in destruction due to the presence of H<sub>2</sub> in the process stream is seen to saturate above a H<sub>2</sub>/NF<sub>3</sub> ratio ( $\alpha$ ) of about 1. More data is needed for  $0 < \alpha < 1$  to determine the precise location of the knee. Figure 6 shows the destruction efficiency of NF<sub>3</sub> as a function of energy density in J/l for  $\alpha=2$ . If one assumes that the relative removal is exponentially dependent on the reactor input energy density as suggested by Rosocha et al<sup>7</sup>, the exponential-folding factor,  $\beta$ , for NF<sub>3</sub> is found to be 320 J/l. Some fall-off in reactor peak voltage at repetition-rates in excess of 1 kHz was noted due to surpassing the recovery characteristics of the H<sub>2</sub> gas in the switch. This slight drop was compensated for by raising the spark-gap gas pressure accordingly.

The chemical performance of the PCR was analyzed for the following pollutant compounds: toluene, methylene chloride, TCA, dichlorodifluoromethane, NF<sub>3</sub>, C<sub>2</sub>F<sub>6</sub>, CF<sub>4</sub>, SF<sub>6</sub>, and NO<sub>2</sub>. With the reactor conditions bounded by 100-300 Watts input power, process-stream flow rates of 5-10 slpm in air or N<sub>2</sub>, pollutant concentrations of a few 100 ppm, and using hydrogen or oxygen as additives, the achieved levels of removal to date are given in Table III. Greater than 99.9% indicates that the detection limits of the GC or MS were surpassed. Delineation of the specific  $\beta$ -factors for each pollutant molecule will be forthcoming in a separate publication.

In order to determine the chemical content of the post-reactor effluent, a series of mass spectrographic static scans were performed for each process gas of interest. Scans were taken of the background gas, the background gas with the PCR running, the background gas plus pollutant and/or additive, and finally with the PCR running in the full process gas stream. These scans were then compared for any changes, with the m/e ratios showing the most significant changes being subsequently monitored during a MS dynamic scan. An analysis of the reaction by-products was performed on four pollutant compounds of principal interest, namely NF<sub>3</sub>, CH<sub>2</sub>Cl<sub>2</sub>, CCl<sub>2</sub>F<sub>2</sub>, and C<sub>7</sub>H<sub>8</sub> as delineated in Table IV. The



principal reaction by-product from the pulsed corona processing of  $\text{NF}_3$  is  $\text{HF}$  which is soluble in water and can easily be removed from the reactor effluent with a water scrubber. For methylene chloride, major by-products appear to be  $\text{Cl}_2$  and  $\text{HCl}$ , with trace amounts of  $\text{HOCl}$  and phosgene ( $\text{COCl}_2$ ). Similarly for  $\text{CCl}_2\text{F}_2$ , major by-products appear to be  $\text{Cl}_2$ ,  $\text{HOCl}$ , and  $\text{COCl}_2$ , except that  $\text{HOCl}$  seems to be more prominent. Fluorine appears primarily in  $\text{COF}^+$ ,  $\text{CF}_2^+$ , and  $\text{CF}_3^+$ . In the case of toluene,  $\text{NO}_x$  was detected as well as a brown residue. This solid product was analyzed by XPS. The residue was found to be a carbonaceous fluoride ( $\text{CF}_x$ ) which is indicative of Teflon, a possible source of which is the reactor pressure seals. Toluene was the only species studied that produced by-products with a higher  $m/e$  than the parent molecule. Ozone was present in all the runs conducted in an air background.

### Conclusions

The fast risetime pulsed corona reactor has been demonstrated as effective against a wide variety of hazardous gaseous compounds including  $\text{NF}_3$ , methylene chloride, toluene, TCA, Freon, and to a lesser extent,  $\text{SF}_6$ ,  $\text{CF}_4$ , and  $\text{C}_2\text{F}_6$ . The use of small concentrations of additives has resulted in a significant increase in the chemical efficacy of the reactor. By-products resulting from the non-thermal plasma treatment of the PFCs have been determined to be water-scrubbable.

Stable operation of the reactor has been demonstrated at voltage up to 35 kV and repetition-rates to 1.5 kHz. The "wall-plug" electrical efficiency of the reactor has been measured to be in excess of 85%. The reactor scheme has proven itself to be quite reliable with over  $10^9$  shots on the hydrogen spark-gap with no discernable degradation in performance.

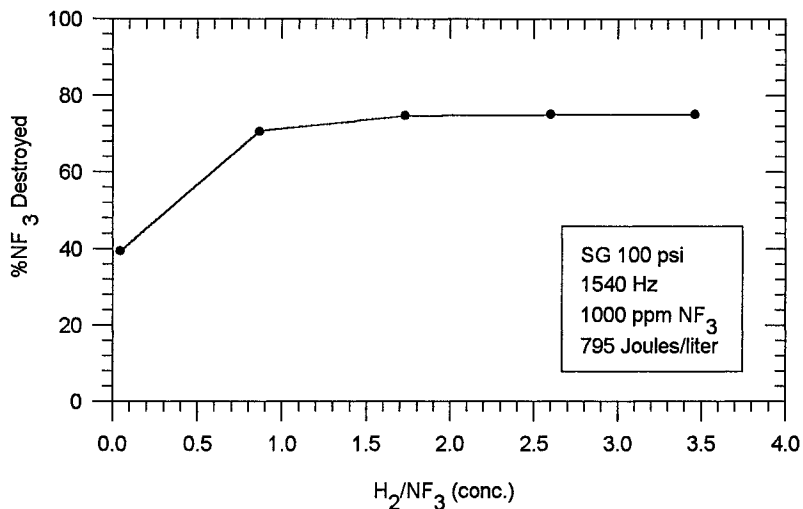


Figure 5. Dependence of  $\text{NF}_3$  destruction on the concentration of hydrogen additive.

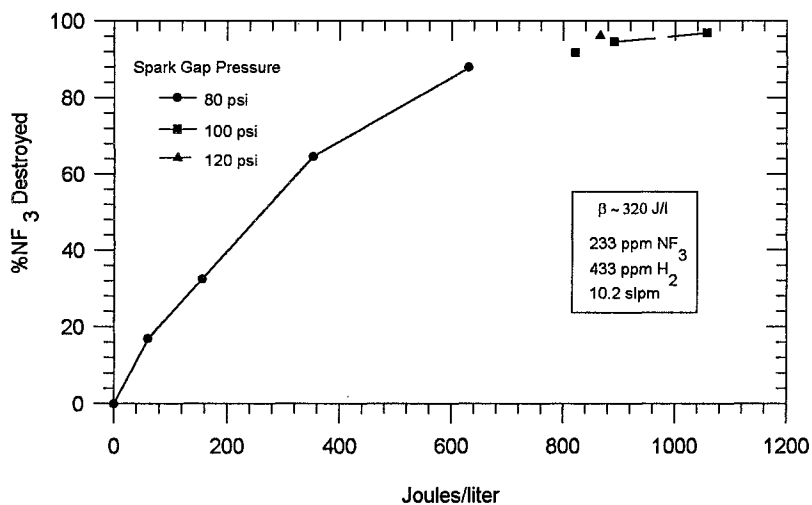


Figure 6. Destruction of 233 ppm  $\text{NF}_3$  as a function of PCR input energy density.

Future efforts will be directed at performing additional electrical, chemical and spectroscopic observations to address some outstanding questions--namely do streamer tip electrons or channel electrons drive reactant production, what is the streamer electron energy distribution, what are the rate-limiting steps in the chemical destruction process.

### Acknowledgements

This work was supported by NAVSEA under the direction of Stan Enatsky, Code 05R. Much of this work was the result of a Cooperative Research and Development Agreement existing between NSWCCD and APCI (NCRADA-NSWCCD-94-006).

### References

- 1) A. Johnson, J. Langan, P. Maroulis, R. Ridgeway, H. Withers, "Review of the Pertinent Technical Information of the Global Warming and Ozone Depletion Potentials of  $\text{NF}_3$ ,"  $\text{NF}_3$  Environmental Task Force, Air Products and Chemicals, Inc., 1993.
- 2) P. Burggraaf, "Process Exhaust Treatment," *Semiconductor International*, April 1993, pp. 44-47.
- 3) *Non-Thermal Plasma Techniques for Pollution Control, Parts A & B*, edited by B. Penetrante and S. Schultheis, NATO ASI Series G: Ecological Sciences, Vol. 34, Part A and B, Springer-Verlag, Heidelberg, 1993.
- 4) B. Eliasson and U. Kogelschatz, "Non-equilibrium Volume Plasma Chemical Processing," *IEEE Trans. on Plasma Science*, Vol. 19, No. 6, Dec. 1991.
- 5) S. Moran and L. Hardesty, "High-Repetition-Rate Hydrogen Spark-Gap," *IEEE Trans. on Electron Devices*, Vol. 38, No. 4, Apr. 1991.
- 6) M. Grothaus, R. Hutcherson, R. Korzekwa, R. Roush, R. Brown, and R. Engels, "Coaxial Pulsed Corona Reactor for Treatment of Hazardous Gases," *Proceedings of the 9th International IEEE Pulsed Power Conference*, Albuquerque, NM, 1993, pp. 180-183.
- 7) L. Rosocha, G. Anderson, L. Bechtold, J. Coogan, H. Heck, M. Kang, W. McCulla, R. Tennant, P. Wantuck, "Treatment of Hazardous Organic Wastes Using Silent Discharge Plasmas," *Non-Thermal Plasma Techniques for Pollution Control: Part B*, pp. 281-308.

Table IV  
Preliminary By-product Identification

Molecule	Destruction By-products
$\text{NF}_3$	$\text{N}_2^+$ , $\text{HF}^+$
$\text{CCl}_2\text{F}_2$	$\text{Cl}_2^+$ , $\text{COCl}^+$ , $\text{O}_3^+$ , $\text{COF}_2^+$ , $\text{CF}_2^+$ $\text{COF}^+$ , $\text{COCIF}^+$
$\text{C}_7\text{H}_8^*$	$\text{CO}_2^+(\text{N}_2\text{O}^+)$ , $\text{H}_2^+$ , $\text{O}_3^+$ , $\text{C}_x\text{H}_y^+$ , $\text{NO}_2^+$ , $\text{C}^+$ , also higher m/e at 105, 106
$\text{CH}_2\text{Cl}_2$	$\text{Cl}_2^+$ , $\text{COCl}^+$ , $\text{O}_3^+$
*Solid product observed and analyzed by XPS C, F, and O components identified. CF <sub>x</sub> component indicative of Teflon.	

Figure 7. Summary of the identified by-products resulting from the non-thermal plasma treatment of a process stream containing hazardous compounds in dilute concentrations.